

## Device for Generating a Low Temperature, Highly Ionized Cesium Plasma

Nathan Rynn and Nicola D'Angelo

Citation: *Review of Scientific Instruments* **31**, 1326 (1960); doi: 10.1063/1.1716884

View online: <http://dx.doi.org/10.1063/1.1716884>

View Table of Contents: <http://scitation.aip.org/content/aip/journal/rsi/31/12?ver=pdfcov>

Published by the **AIP Publishing**

---

### Articles you may be interested in

[Negative ion production in cesium seeded high electron temperature plasmas](#)

*Rev. Sci. Instrum.* **79**, 02C112 (2008); 10.1063/1.2823899

[Dissociative recombination coefficient for low temperature equilibrium cesium plasma](#)

*J. Appl. Phys.* **92**, 690 (2002); 10.1063/1.1486250

[Highly Ionized Dense Plasma in a Cesium Penning Arc](#)

*Phys. Fluids* **8**, 1550 (1965); 10.1063/1.1761452

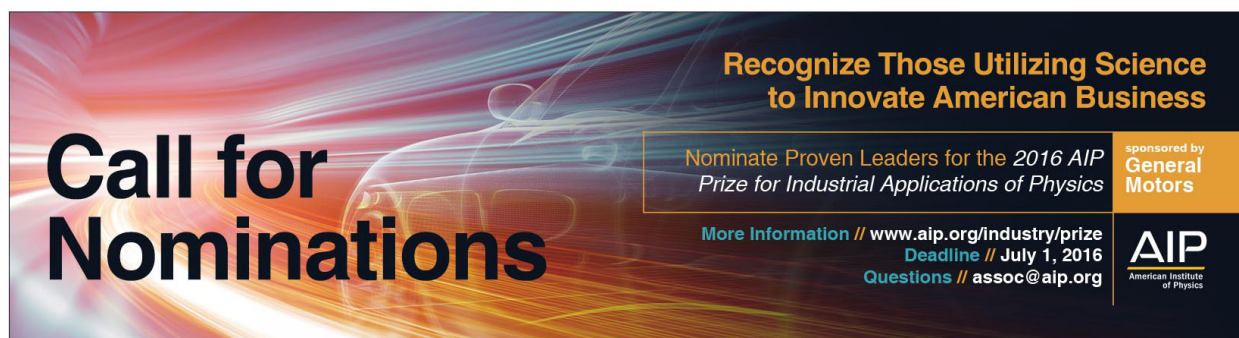
[An Ionization Process in a Low-Energy Cesium Plasma](#)

*J. Appl. Phys.* **36**, 1328 (1965); 10.1063/1.1714305

[Loss of Plasma from Cesium Devices](#)

*Phys. Fluids* **8**, 205 (1965); 10.1063/1.1761094

---



**Call for Nominations**

**Recognize Those Utilizing Science to Innovate American Business**

Nominate Proven Leaders for the *2016 AIP Prize for Industrial Applications of Physics*

More Information // [www.aip.org/industry/prize](http://www.aip.org/industry/prize)  
Deadline // July 1, 2016  
Questions // [assoc@aip.org](mailto:assoc@aip.org)

sponsored by  
**General Motors**

**AIP**  
American Institute of Physics

## Device for Generating a Low Temperature, Highly Ionized Cesium Plasma\*

NATHAN RYNN AND NICOLA D'ANGELO

*Project Matterhorn, Princeton University, Princeton, New Jersey*

(Received July 25, 1960)

A device for generating a linear, highly ionized, low temperature cesium plasma is described. The plasma is generated by having the output of cesium atomic beam ovens impinge on hot tungsten plates placed at both ends of a cylindrical vacuum chamber. The walls of the chamber are cooled so that neutral cesium condenses on them. The theory of the device, designated as the Q machine, is presented and some experimental results given. The maximum density achieved was  $2 \times 10^{12}/\text{cm}^3$ , with an estimated fractional ionization of 99%, and a confining field of 5900 gauss.

### I. INTRODUCTION

THIS paper is concerned with the problem of making a quiescent plasma with properties of interest to workers in the fields of plasma physics, controlled thermonuclear reactions, and astrophysics. It was decided that the plasma should have a low temperature in order to avoid the necessity of first solving a difficult containment problem.<sup>1</sup> The common method of using an electrical discharge to produce it invariably creates disturbances which are hard to control and difficult to understand. We have found that contact ionization of cesium on hot tungsten,<sup>2-4</sup> coupled with containment in a magnetic field, is a satisfactory means of producing the desired plasma.

Figure 1 shows a schematic drawing of the device. Hot tungsten plates are mounted at both ends of an evacuated chamber. Associated with each plate is an atomic beam oven, containing cesium. Each oven is oriented so that its beam impinges on, or "illuminates," the hot tungsten plate. The vacuum chamber walls can be maintained at a temperature less than that of the plates, and the entire device is placed inside a solenoid which produces a uniform magnetic field. The gas need not be cesium vapor, nor the hot plates tungsten. Various combinations will work as long as the ionization potential of the gas is less than the work function of the hot plate. For convenience, however, we shall speak of cesium on tungsten.

The basic principle is that the monatomic cesium vapor is singly ionized by the hot tungsten which is also hot enough to emit electrons in sufficient quantities to ensure charge neutrality. A thin sheath, whose properties will depend on the balance between ions and electrons, will form on each plate. Beyond the sheath region will be an essentially neutral plasma contained in the radial direction by the magnetic field. There are two possible modes of

operation. One we shall designate as the vapor pressure mode and the other as the atomic beam mode. The vapor pressure mode is formed by introducing metallic cesium into the vacuum chamber. This can be done either by turning on the beam ovens for a short period or by dispensing with them and introducing metallic cesium into the vacuum chamber. The vacuum chamber is sealed off and the vapor pressure of the cesium is controlled by the temperature of the walls. The vapor pressure, in turn, determines the number of cesium neutrals striking the plates and, thereby, determines the plasma density. In the atomic beam mode, the chamber walls are cooled so that cesium neutrals condense on them and are rapidly pumped out of the plasma. The cesium neutrals are delivered to the hot plates by means of the atomic beam ovens. Since the neutral background can be made quite small by this method, this mode is inherently capable of higher percentage ionizations than the vapor pressure mode.

A theoretical analysis is presented in Sec. II. First, a one-dimensional case is considered and then the three-dimensional case is discussed. The relative advantages and disadvantages of both modes of operation are also discussed. Section III describes the Q machine, the designation of the actual device built at Project Matterhorn. Section IV describes some measurements taken with the Q machine, and Sec. V discusses the results.

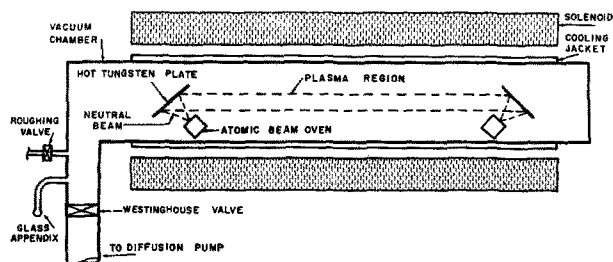


FIG. 1. Schematic drawing of the Q machine, the designation of the cesium plasma source at Project Matterhorn. The vacuum chamber walls are cooled by means of a water jacket. Cesium atomic beams impinging on hot tungsten plates form the plasma which is contained by the magnetic field of the solenoid. The tungsten plates are 50 cm apart.

\* This work was supported under contract with the U. S. Atomic Energy Commission.

<sup>1</sup> A. S. Bishop, *Project Sherwood* (Addison-Wesley Publishing Company, Inc., Reading, Massachusetts, 1958).

<sup>2</sup> I. Langmuir and K. H. Kingdon, *Proc. Royal Soc. (London)* **A107**, 61 (1925).

<sup>3</sup> J. B. Taylor and I. Langmuir, *Phys. Rev.* **44**, 423 (1933).

<sup>4</sup> H. G. Hernqvist, M. Kanefsky, and F. H. Norman, *RCA Rev.* **19**, 244 (1958).

## II. THEORY

Figure 2 shows an idealization of Fig. 1. Two identical circular tungsten disks of radius  $r_2$  are placed at distances  $\pm \frac{1}{2}L$  from the origin. The plates, which have a common axis, are "illuminated" by the neutral cesium beams out to a radius  $r_1$ . The magnetic field of intensity  $B_0$  is uniform and parallel to the  $z$  axis. We assume that hot tungsten is a perfect (diffuse) reflector for cesium ions.<sup>5</sup> We assume that the sheath is very thin<sup>6</sup> and that the plasma flux just outside the sheath is the same as the incoming neutral flux at the surface of the plates.

Reference to a basic work in plasma physics<sup>7</sup> will show that for a fully ionized cesium plasma of a density of  $10^{12}/\text{cm}^3$ , and a temperature of  $2000^\circ\text{K}$ , the electron-ion collision distance is of the order of 1 mm. With this in mind, we write the Boltzmann equations for ions and electrons as

$$\frac{\partial f_i}{\partial t} + \mathbf{w}_i \cdot \nabla f_i + \mathbf{a}_i \cdot \nabla_{\mathbf{w}} f_i = \left( \frac{\delta f_i}{\delta t} \right)_{\text{coll}} - \left( \frac{\delta f_i}{\delta t} \right)_{\text{recomb}} \quad (1a)$$

$$\frac{\partial f_e}{\partial t} + \mathbf{w}_e \cdot \nabla f_e + \mathbf{a}_e \cdot \nabla_{\mathbf{w}} f_e = \left( \frac{\delta f_e}{\delta t} \right)_{\text{coll}} - \left( \frac{\delta f_e}{\delta t} \right)_{\text{recomb}}, \quad (1b)$$

where  $f_i(\mathbf{r}, \mathbf{w}, t)$  and  $f_e(\mathbf{r}, \mathbf{w}, t)$  represent the ion and electron distribution functions, respectively;  $\mathbf{r}$  is the position vector,  $\mathbf{w}$  the velocity vector, and  $t$  is the time.

The last term in each equation represents the loss of particles due to recombination. For the ions, this may be written as

$$\begin{aligned} \left( \frac{\delta f_i}{\delta t} \right)_{\text{recomb}} &= f_i(x, y, z, \xi, \eta, \zeta, \lambda, \mu, \nu) \\ &\times \int_{-\infty}^{\infty} \int_{-\infty}^{\infty} \int_{-\infty}^{\infty} \alpha' [(\xi - \lambda)^2 + (\eta - \mu)^2 + (\zeta - \nu)^2] \\ &\times f_e(x, y, z, \lambda, \mu, \nu, t) d\lambda d\mu d\nu, \quad (2) \end{aligned}$$

where  $\xi, \eta, \zeta$  are the components of the ion velocity vector;  $\lambda, \mu, \nu$  are the components of the electron velocity vector; and,  $\alpha'$  is a constant of proportionality that is a function of the absolute magnitude of the relative velocity of the two particles. Equation (2) can be rewritten as

$$\left( \frac{\delta f_i}{\delta t} \right)_{\text{recomb}} = f_i(x, y, z, \xi, \eta, \zeta, t) \bar{\alpha}'(\xi, \eta, \zeta) n_e(x, y, z, t), \quad (3)$$

<sup>5</sup> This assumption is usually justified on the grounds that the cesium ion is adsorbed on the hot tungsten and reionized when it is evaporated off; cf. Langmuir and Kingdon.<sup>2</sup>

<sup>6</sup> Compare H. Dreicer, "Plasma in equilibrium," Proc. Conf. Controlled Thermonuclear Reactions (Princeton, New Jersey, October 1955), pp. 507-511, TID-7503.

<sup>7</sup> See, for example, L. Spitzer, Jr. *Physics of Fully Ionized Gases* (Interscience Publishers, Inc., New York, 1956).

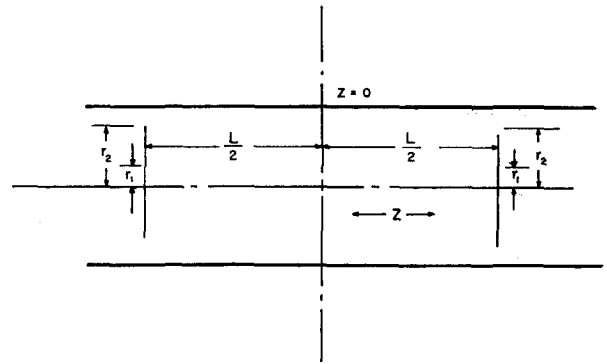


FIG. 2. Idealization of the Q machine.

where  $n_e$  is the electron density and  $\bar{\alpha}'$  is the average of  $\alpha'$  over the electron velocity distribution. If we make the substitution

$$\mathbf{w}_{i,e} = \mathbf{u}_{i,e} + \mathbf{v}_{i,e},$$

where  $\mathbf{u}$  represents the random velocity component of  $\mathbf{w}$ ,  $\mathbf{v}$  is the drift velocity, and the subscripts  $i$  and  $e$  refer to ions and electrons, respectively, and integrate Eq. (1a) over the ion velocities, the result is

$$(\partial n_i / \partial t) + \nabla \cdot (n_i \mathbf{v}_i) + \alpha n_i n_e = 0, \quad (4)$$

where  $n_i$  is the ion density and  $\alpha$  is the usual recombination coefficient.

We take the first moment of Eq. (1a) by multiplying by  $m_i \mathbf{w}_i$ , where  $m_i$  is the ion mass, and again integrating over the ion velocities. By noting that  $\mathbf{u}_i = 0$ , this results in the momentum equation,

$$\begin{aligned} n_i m_i \frac{\partial \mathbf{v}_i}{\partial t} + \mathbf{v}_i \frac{\partial (n_i m_i)}{\partial t} + n_i m_i \mathbf{v}_i \cdot \nabla \mathbf{v}_i + \mathbf{v}_i \nabla \cdot (n_i m_i \mathbf{v}_i) \\ + \nabla \cdot \Psi_i - n_i q (\mathbf{E} + \mathbf{v}_i \times \mathbf{B}) = \mathbf{P}_{ie} - m_i n_e n_i \alpha \mathbf{v}_i, \quad (5) \end{aligned}$$

where  $\Psi$  is the ion stress tensor,  $q$  is the electron charge,  $\mathbf{E}$  the electric field vector,  $\mathbf{B}$  the magnetic field vector, and  $\mathbf{P}_{ie}$  is the total momentum transferred to the ions per unit volume per unit time by collisions with the electrons. A similar treatment applies to Eq. (1b). We note that, after Spitzer,<sup>7</sup>

$$\mathbf{P}_{ie} = -\mathbf{P}_{ei} = -\eta q^2 n_e (n_i \mathbf{v}_i - n_e \mathbf{v}_e), \quad (6)$$

where  $\eta$  is the electrical resistivity. We make the assumption that the stress tensors may be replaced by  $(n_i, e k T_{i,e})$ , where  $k$  is the Boltzmann constant and  $T_{i,e}$  is the ion or electron temperature and is assumed constant. When the momentum equations are simplified by substituting into them the continuity equations, and time independent solutions are looked for, the final result is

$$\nabla \cdot (n_i \mathbf{v}_i) + \alpha n_i n_e = 0 \quad (7a)$$

$$\nabla \cdot (n_e \mathbf{v}_e) + \alpha n_i n_e = 0 \quad (7b)$$

$$n_i m_i \mathbf{v}_i \cdot \nabla \mathbf{v}_i + kT_i \nabla n_i - n_i q(\mathbf{E} + \mathbf{v}_i \times \mathbf{B}) = -\eta q^2 n_e (n_i \mathbf{v}_i - n_e \mathbf{v}_e) \quad (7c)$$

$$n_e m_e \mathbf{v}_e \cdot \nabla \mathbf{v}_e + kT_e \nabla n_e + n_e q(\mathbf{E} + \mathbf{v}_e \times \mathbf{B}) = \eta q^2 n_e (n_i \mathbf{v}_i - n_e \mathbf{v}_e). \quad (7d)$$

Note that the recombination term has been eliminated from the momentum equations. The reason for this is that the neutral atom resulting from recombination carries away with it the full momentum of the electron-ion pair.

### A. One-Dimensional Case

To make the problem one dimensional let  $r_1$  and  $r_2$  in Fig. 2 go to infinity. Equations (7) become

$$\frac{d}{dz}(n_i v_i) + \alpha n_i n_e = 0 \quad (8a)$$

$$\frac{d}{dz}(n_e v_e) + \alpha n_i n_e = 0 \quad (8b)$$

$$n_i m_i v_i \frac{dv_i}{dz} + kT_i \frac{dn_i}{dz} - qn_i E = -\eta q^2 n_e (n_i v_i - n_e v_e) \quad (8c)$$

$$n_e m_e v_e \frac{dv_e}{dz} + kT_e \frac{dn_e}{dz} + qn_e E = +\eta q^2 n_e (n_i v_i - n_e v_e). \quad (8d)$$

On subtracting Eq. (8b) from Eq. (8a), and integrating, the result is

$$n_i v_i - n_e v_e = 0, \quad (9)$$

where we have used the condition that

$$[v_e]_{z=0} = [v_i]_{z=0} = 0 \quad (10)$$

because of symmetry. Using this result in Eqs. (8c) and (8d), dividing the former by  $n_i$ , the latter by  $n_e$ , adding and integrating, we get

$$n_i n_e = n_{i0} n_{e0} \exp[-(1/2kT)(m_i v_i^2 + m_e v_e^2)], \quad (11a)$$

where we have assumed that

$$T_e = T_i = T$$

and  $n_{i0}$  and  $n_{e0}$  are the ion and electron densities at  $z=0$ . Invoking plasma neutrality and Eq. (9), we have the relationship

$$m_i v_i^2 \gg m_e v_e^2.$$

Equation (11a) becomes

$$n = n_0 \exp(-m_i v_i^2 / 4kT). \quad (11b)$$

Substitution of Eq. (11b) into the continuity equation gives

$$\left(1 - \frac{m_i v_i^2}{2kT}\right) \frac{dv_i}{dz} + \alpha n_0 \exp\left(\frac{-m_i v_i^2}{4kT}\right) = 0. \quad (12)$$

This equation can be integrated numerically to give  $v_i$  as a function of  $z$ . Putting the resulting relationship in Eq. (11b) will give the axial profile. It is not necessary to solve these equations in detail.

For the condition

$$m_i v_i^2 / 2kT \ll 1 \quad (13)$$

it follows that

$$v_i = -\alpha n_0 z; \quad (14)$$

and, from Eq. (11b)

$$n = n_0 \exp[-m_i (\alpha n_0 z)^2 / 4kT]. \quad (15)$$

This predicts a density profile with a density maximum at the center. Note also that when condition (13) holds as, for example, in the experimental situation described later, the axial density gradient is very small.

For design purposes, it is important that the limits of applicability of Eqs. (13)–(15) be determined. This can be done by a closer examination of Eq. (12). So long as

$$m_i v_i^2 / 2kT < 1, \quad (16)$$

$dv_i/dz$  is negative and the conclusion previously arrived at applies. For

$$m_i v_i^2 / 2kT > 1, \quad (17)$$

however, the entire nature of the solution changes. We shall now attempt to determine the conditions under which Eq. (16) applies. Rewrite Eq. (12) as

$$\left[\left(1 - \frac{m_i v_i^2}{2kT}\right) \exp\left(\frac{m_i v_i^2}{4kT}\right)\right] \frac{dv_i}{dz} + \alpha n_0 = 0. \quad (18)$$

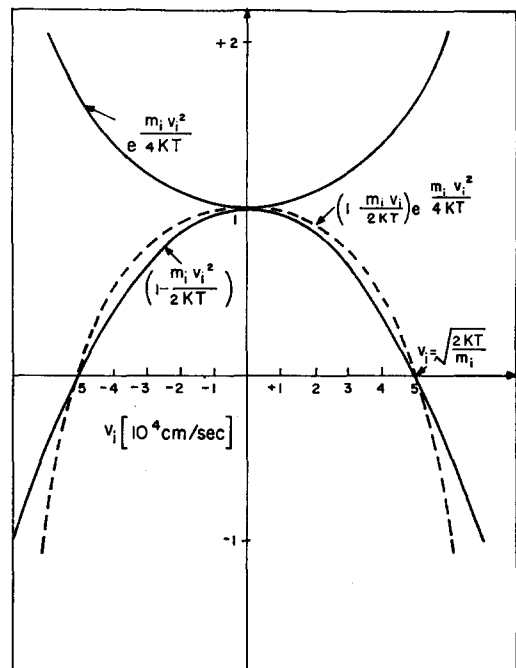


FIG. 3. A plot of  $[1 - (m_i v_i^2 / 2kT)] \exp(m_i v_i^2 / 4kT)$  and their product. These curves are useful in determining limiting dimensions.

Figure 3 shows a plot of  $[1 - (m_i v_i^2/2kT)]$ ,  $[\exp(m_i v_i^2/4kT)]$  and their product. We define the function

$$\Phi_T(v_i) \equiv \int_0^{v_i} \left(1 - \frac{m_i v_i^2}{2kT}\right) \exp(m_i v_i^2/4kT) dv_i, \quad (19)$$

a plot of which is shown in Fig. 4.  $\Phi_T$  has a relative minimum at  $v_i = -(2kT/m_i)^{1/2}$  and a relative maximum at  $v_i = (2kT/m_i)^{1/2}$ . We confine our attention to the  $z < 0$  portion of Fig. 2 so that  $\Phi_T$  will have a positive value. The maximum value of  $\Phi_T$ ,  $M_T$ , must be

$$M_T \geq \alpha n_0 L/2. \quad (20)$$

By making use of Eq. (11b),

$$M_T \geq \alpha \frac{L F}{2 v_L} \exp(m_i v_L^2/4kT), \quad (21)$$

where  $n_L$  and  $v_L$  are the density and drift velocity at  $-\frac{1}{2}L$ , and  $F$  is the flux of neutrals, assuming every neutral gets ionized, at each one of the two end plates. The right-hand side of Eq. (21) has a minimum at

$$v_L = (2kT/m_i)^{1/2},$$

and a value at that point of

$$e^{1/2} (m_i/2kT)^{1/2} (\alpha L F/2).$$

On putting this result into Eq. (21),

$$M_T \geq \alpha (L/2) F e^{1/2} (m_i/2kT)^{1/2}. \quad (22)$$

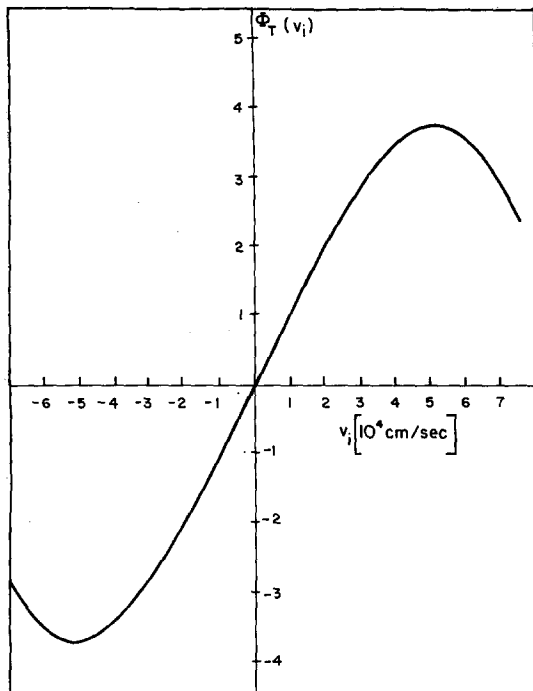


FIG. 4. A plot of a function,  $\Phi_T(v_i)$ , useful in determining machine dimensions.

For given values of  $T$ ,  $\alpha$ , and  $F$ , Eq. (22) gives the maximum length of the machine for which the foregoing theory applies. The inequality (22) may be rewritten

$$\int_0^1 (1 - \xi^2) \exp\left(\frac{\xi^2}{2}\right) d\xi \geq \frac{L}{2} F e^{1/2} \left(\frac{m_i}{2kT}\right)^{1/2} \alpha, \quad (23)$$

where  $\xi$  is a dimensionless variable. The value of the integral is of the order of unity, as is  $e^{1/2}$ , so that

$$\alpha L F (m_i/4kT) \sim 1. \quad (24)$$

For  $n_0 = 10^{12}/\text{cm}^3$ , and our design values ( $\alpha = 3 \times 10^{-10}$   $\text{cm}^3/\text{sec}$ ;  $T = 2000^\circ\text{K}$ ),  $F \sim 10^{16}$   $\text{cm}^2/\text{sec}$ . For this value of  $F$  the maximum  $L$  for which the theory applies is of the order of 3 m.

## B. Radial Profile

To extend the analysis to the three-dimensional case and keep it within practical bounds, it is necessary to make certain approximations and assumptions. The first of these is that the  $\mathbf{v} \cdot \nabla \mathbf{v}$  term in Eq. (7) is negligible. This can be justified by a closer examination of the one-dimensional case for the design values previously assumed. The hypothesis of complete ionization carries with it the implication that the radial diffusion is ambipolar,<sup>8</sup> i.e., that the ion and electron radial drift velocities are equal. This being so, and since the ions and electrons recombine at the same rate, the same conclusion applies to the axial drift velocities. Accordingly,  $\mathbf{v}_i$  and  $\mathbf{v}_e$  can differ only in their  $\theta$  components. The electric field,  $\mathbf{E}$ , is taken to be zero everywhere. This is justified on the grounds that in the body of the plasma there is no mechanism available to create the necessary charge buildup. At the edge of the plasma, where the density is low, the "Simon short-circuit effect"<sup>8</sup> will tend to keep fields from building up as a consequence of the geometry that we have chosen.

We use all the assumptions in Eq. (7) and add to the set the Maxwell equation,

$$\nabla \times \mathbf{B} = 4\pi \mathbf{j},$$

where  $\mathbf{j}$  is the current density. In cylindrical coordinates the result is

$$\frac{1}{r} \frac{\partial}{\partial r} (r n v_r) + \frac{\partial}{\partial z} (n v_z) + \alpha n^2 = 0 \quad (26a)$$

$$2kT \frac{\partial n}{\partial r} - q n (v_{i\theta} - v_{e\theta}) B = 0 \quad (26b)$$

$$\partial n / \partial z = 0 \quad (26c)$$

$$q (v_{i\theta} + v_{e\theta}) B = 0 \quad (26d)$$

$$-2q n v_r B = 2\eta q^2 n^2 (v_{i\theta} - v_{e\theta}) \quad (26e)$$

$$-\partial B / \partial r = 4\pi q n (v_{i\theta} - v_{e\theta}), \quad (26f)$$

<sup>8</sup> A. Simon, *An Introduction to Thermonuclear Research* (Pergamon Press, New York, 1959).

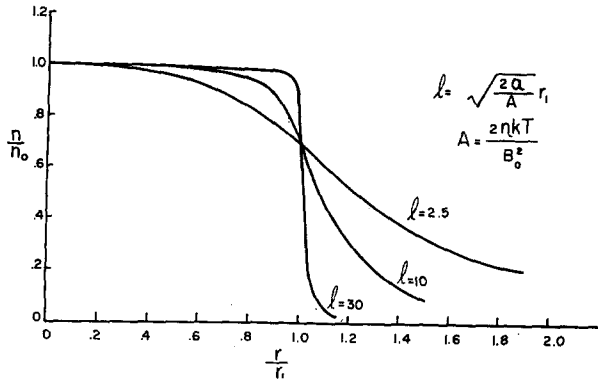


FIG. 5. Calculated radial density profiles for different value of  $l$ , a parameter proportional to the magnetic field. It is assumed that neutrals strike the plate up to a radius  $r_1$ , and that the plate diameter is infinite.

where we have assumed that there are no  $\theta$  variations. Equation (26d) tells us that the two  $\theta$  drift velocities are equal and opposite; Eq. (26c) is a consequence of the neglect of  $\mathbf{v} \cdot \nabla \mathbf{v}$ .

It is easy to show from Eqs. (26) that

$$nkT + (B^2/16\pi) = B_0^2/16\pi, \quad (27)$$

where  $B_0$  is the external magnetic field. From this it follows that  $B$ ,  $n$ ,  $v_r$ ,  $v_\theta$ , and  $\partial v_z/\partial z$  depend only on  $r$ . Since  $v_z=0$  at  $z=0$ , we may write

$$v_z(r,z) = f(r)z, \quad (28)$$

where  $f(r)$  depends only upon  $r$  and is yet to be determined.

The plasma "self-field" is negligible so that  $B$  can be taken equal to the external field. It will also be found that

$$16\pi kTn/B_0^2 \ll 1.$$

Since the incoming flux of neutrals must be equal to the flux of ions supplied to the plasma, we have, at one end, by Eq. (28), that

$$(nv)_{\text{neutrals}} = \left[ \frac{1}{2} nL f(r) \right].$$

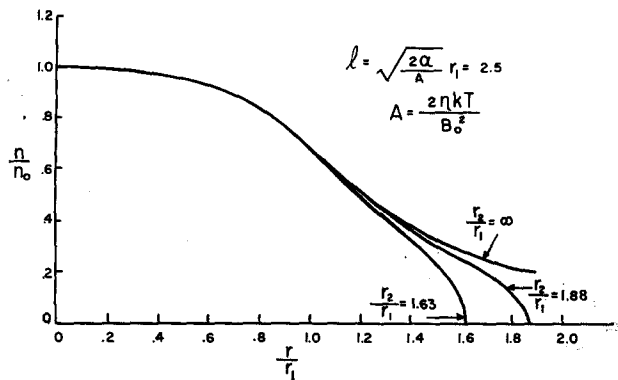


FIG. 6. Calculated radial density profiles for a particular value of the parameter  $l$  showing the effect of finite plate radius. For  $r_2/r_1 = 1.88$ , the density profile coincides with that for  $r_2 = \infty$  out to  $r/r_1 = 1.25$ .

Hence, it is clear that  $nf(r)$  is determined by the incoming stream of neutrals. For the atomic beam mode, the radial distribution of neutrals is, in principle, at the disposal of the experimenter. Suppose we assume that, referring to Fig. 2,

$$nf(r) = \mu \quad \text{for } 0 \leq r \leq r_1 \quad (\text{region I})$$

$$nf(r) = 0 \quad \text{for } r_1 \leq r \leq r_2 \quad (\text{region II}),$$

Eqs. (26) become

$$\frac{d^2(n^2)}{dr^2} + \frac{1}{r} \frac{d(n^2)}{dr} - \frac{2\alpha}{A} n^2 = -\frac{2\mu}{A} \quad (\text{region I}), \quad (29a)$$

$$\frac{d^2(n^2)}{dr^2} + \frac{1}{r} \frac{d(n^2)}{dr} - \frac{2\alpha}{A} n^2 = 0 \quad (\text{region II}), \quad (29b)$$

where

$$A = 2\eta kT/B_0^2.$$

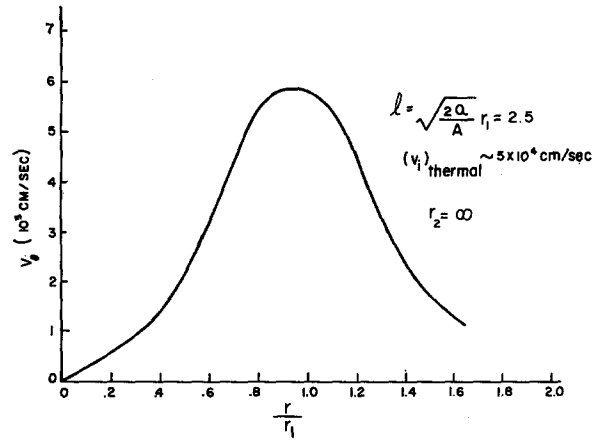


FIG. 7. A calculated plot of the rotational velocity  $v_\theta$ , as a function of the radius, for a particular value of the parameter  $l$ . The maximum value is about  $1/10$  of the thermal velocity and occurs at  $r/r_1 = 0.95$ .

The solutions to Eqs. (29) have the form of zero-order Bessel functions<sup>9</sup> of argument  $il(r/r_1)$ , where

$$l \equiv r_1(2\alpha/A)^{1/2}.$$

Region I requires Bessel functions of the first kind, region II requires the first and second kinds unless  $r_2 = \infty$ , in which case only the second kind is needed. The boundary conditions are that  $n = n_0$  at  $r = 0$ ; that the densities and their radial derivatives match at  $r = r_1$ ; and that  $n = 0$  at  $r = r_2$ . Solutions to Eqs. (29) for various values of  $l$  are shown in Fig. 5 for the case where  $\eta = 4.4 \times 10^8$  emu,  $T = 2000^\circ\text{K}$ , and  $r_2 = \infty$ . The effect of finite  $r_2$  is shown in Fig. 6. Note that the density profiles approximate that of  $r_2/r_1 = \infty$ , for most of the plate area illuminated, for the values shown.

<sup>9</sup> E. Janke and F. Emde, *Tables of Functions* (G. E. Stechert & Company, New York, 1938), 3rd ed.

From Eq. (29b) the rotational velocity  $v_\theta$  as a function of  $r/r_1$ , has been plotted in Fig. 7 for  $B_0=2000$  gauss and  $\alpha=3\times 10^{-10}$  cm<sup>3</sup>/sec. The maximum value of  $6\times 10^8$  cm/sec, about one-tenth the thermal speed, is attained near  $r/r_1=1$ .

### C. Some Design Considerations

We can now make certain statements about the prospective machine. For one, the total length of the plasma should be less than 3 m for a density of  $10^{12}$ /cm<sup>3</sup> if we wish the foregoing theory to apply. For another, it would be interesting to compare the vapor pressure mode with the atomic beam mode. It is clear that the atomic beam mode can be made to give a very high degree of ionization, tailor-made profiles, etc. However, the use of atomic beams increases the complexity of the machine since they require periodic reloading with cesium, accurate alignment, etc. On the other hand, the vapor pressure mode requires only the introduction of metallic cesium, automatically "illuminates" the plates uniformly, etc. However, only one fractional ionization is possible at a given density.

Examination of Eqs. (29) and Fig. 5 will show that for confining fields of the order of 2000 gauss or higher, particle loss is due mainly to recombination. Accordingly, we can approximate the necessary input neutral flux by multiplying the recombination rate by the plasma volume. For an  $\alpha=3\times 10^{-10}$  cm<sup>3</sup>/sec,  $n=10^{12}$ /cm<sup>3</sup>, and a length of 10 cm, a flux of  $1.5\times 10^{15}$  neutrals cm<sup>2</sup>/sec is required. From vapor pressure curves for cesium it can be shown that this corresponds to a cesium neutral background of about  $10^{11}$ /cm<sup>3</sup> or a fractional ionization of about 90%. For a 50 cm length of plasma, this value becomes about 70%, for 1 m it becomes about 50%. For higher densities the percentage ionization possible becomes lower, for lower densities it becomes higher. Thus, the vapor pressure mode seems useful for small volume plasmas, such as may be put into sealed-off tubes, or for those cases where a high fractional ionization is not necessary. Note also that the boundary conditions at the edge of the plasma in this mode are not clear. Experiments of interest in the controlled thermonuclear reaction field usually require large volumes of plasma, very high percentage ionizations, and well-defined boundary conditions, indicating the atomic beam mode for this application.

### III. Q MACHINE

The machine that was built at Project Matterhorn to embody the ideas thus far discussed has been designated as the Q machine. The solenoid coils are spaced so as to give a variation of the  $B$  field of not more than 5% over the length of the machine and yet allow access to the center section for diagnostic instrumentation. The magnetic field can be varied from a minimum of 200 gauss to

a maximum of 7000 gauss for continuous operation, or to 10 000 gauss for a short period. The vacuum vessel has been fabricated of nonmagnetic stainless steel, in sections, and gasketed with gold seals to allow baking. A cooling jacket surrounds the entire chamber. With well water as the coolant, the temperature of the vacuum chamber wall is held to 15°C while the tungsten plates are hot. Although the tungsten plates are shown 50 cm apart, they can be mounted anywhere in the tube. The system can also be operated "single-ended," i.e., with only one hot plate at one end and a cold collector at the other. The diagnostic section contains four "cross-ports." Two in one plane are taken up by 8-mm microwave horns. There are two more ports in a plane at right angles to the horns, one of which contains a glass viewing port and the other a Langmuir probe. The Langmuir probe has a bellows arrangement that allows the plasma to be probed in its radial dimension. The end flanges have viewing ports. Electrical connections are brought through the side ports at the ends. The entire system can be baked, by means of externally wrapped heaters, to 350°C.

A 2-in. high vacuum Westinghouse bakable valve has been inserted, as shown in Fig. 1, to allow roughing out of the work chamber and recapture of cesium metal when necessary. The roughing-valve is of the bakable Granville-Phillips type. By closing the Westinghouse valve, the entire system can be baked so that cesium which has condensed on the walls can be driven into the glass appendix. This, in turn, is kept cool during this process by means of a temperature-controlled bath. When all the cesium has been driven out, the glass appendix containing it can be sealed and removed, if desired, by standard glass-working technique.

The tungsten plates are heated by electron bombardment. All the heaters are fed with dc to prevent their destruction by vibration in the strong magnetic field. The tungsten plate is held at a 45° angle and is elliptical in shape so that its projection will be a circle of 2.9 cm in diameter. The bombardment heater is carefully shielded to avoid stray fields in the plasma region.

The cesium ovens are in two sections. One section contains calcium metal and cesium chloride in an intimate mixture. When this mixture is brought up to 400°C or higher, a chemical reaction occurs in which the calcium replaces the cesium to form metallic cesium vapor and calcium chloride. The rate of cesium flow can be controlled by the reaction rate, which is a function of temperature. The cesium vapor travels through the connecting tube to the diffuser, the essential part of which is a tantalum foil which has been precisely corrugated and then wound up so as to give the effect of hundreds of little tubes of about 0.020 in. diameter and a length of 0.250 in., all stacked together and precisely aligned. Each little tube collimates

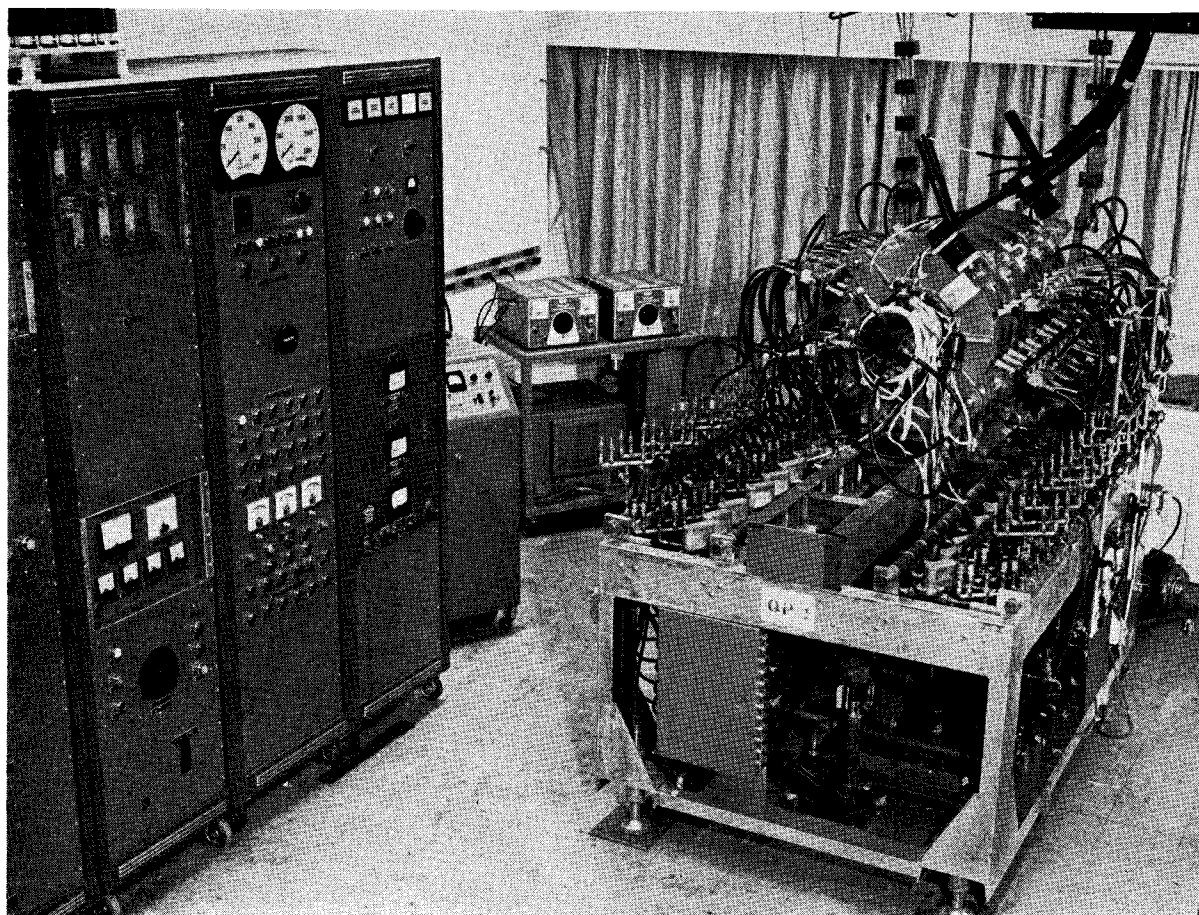


FIG. 8. Photograph of the Q machine.

the cesium vapor into a beam so that the over-all effect is a thick, collimated cesium beam directed at the tungsten plate and centered on it. The beam is made elliptical in cross section by means of an appropriately placed mask. The ellipse dimensions are such that the area it "illuminates" on the tungsten plate projects out as a 2-cm diam

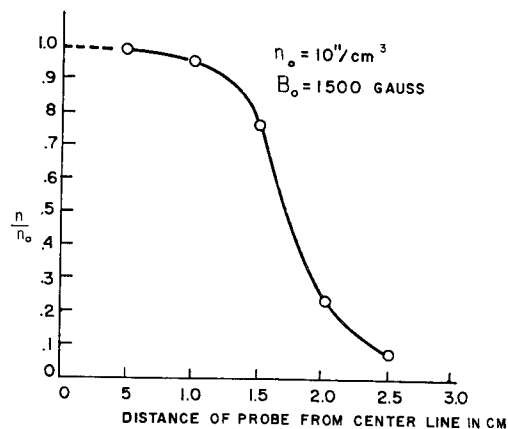


FIG. 9. Plot of a density profile taken with a Langmuir probe on the Q machine. Maximum density was  $10^{11}/\text{cm}^3$ , and the confining field was 1500 gauss.

circle centered on the 2.9-cm diam circle of the tungsten plate.

Figure 8 is a photograph of the machine.

#### IV. MEASUREMENTS TAKEN WITH THE MACHINE

Profile measurements were taken with the Langmuir probe at various densities and various confining fields. Figure 9 shows a plot taken with both plates hot and a plasma density of  $10^{11}/\text{cm}^3$ , and a confining field of 1500 gauss. At a density of  $10^{12}/\text{cm}^3$ , 8-mm microwave measurements were taken and these agreed well with probe measurements. The maximum plate temperature we have used was  $2500^\circ\text{C}$ . The maximum length of plasma was about one meter at  $10^{11}/\text{cm}^3$  under single-ended operation. The maximum measured density was  $2 \times 10^{12}/\text{cm}^3$ , with a fractional ionization of 99%, estimated on the basis of a base pressure of  $10^{-6}$  mm Hg and a wall temperature of  $13^\circ\text{C}$ .

#### V. DISCUSSION

The Q machine was intended to be a versatile machine capable of many types of experiments. The first one, the



theory of which is given in Sec. II, is a check of the so-called classical theory of diffusion of charged particles across a magnetic field. There is considerable general interest in this problem, and its experimental resolution requires more care and better techniques than those used to obtain the data presented. Our immediate objective was to establish that the machine was capable of producing a satisfactory plasma. No particular care was taken to see that the tungsten plates were precisely aligned on their axes or the axes with the magnetic field. The temperature at the center of the plates was higher than that at the edges. The shape and location of the neutral beams were not precisely known, except that we believe that they illuminated the entire area of the plates. We verified that the plasma was indeed attributable to contact ionization of cesium by measuring zero density with the plates hot and the ovens cool. We hope to present more quantitative data, taken

with more accurately constructed components, at a later date.

We believe that we have demonstrated that the Q machine generates a cesium plasma, that the plasma is confined, that we have achieved a high density with a high percentage of ionization, and that, in short, the machine is operating properly and can be used to perform experiments in the field of plasma physics.

#### VI. ACKNOWLEDGMENTS

The authors would like to acknowledge conversations with W. Hooke of the Experimental Physics Division and with J. Dawson and C. Oberman of the Theoretical Physics Division. They would also like to thank A. G. Wentzel, S. Wood, and J. Lidzinski for their help with the electrical and mechanical details, and O. Kraus and his men for their long hours of hard work. Finally, they would like to thank C. Tsipis for his able assistance.